Defining a Slurry Phase Map for Gas Hydrate Management in Multiphase Flow Systems

Carlos Lange-Bassani, Jean-Michel Herri, Ana Cameirão, Rigoberto E. M. Morales, Amadeu K. Sum

Defining a Slurry Phase Map for Gas Hydrate Management in Multiphase Flow Systems

Carlos L. Bassani[†,‡], Jean-Michel Herri[†], Ana Cameirão[†], Rigoberto E.M. Morales[‡*], Amadeu K. Sum[#*]*

[†]Mines Saint-Etienne, Univ Lyon, CNRS, UMR 5307 LGF, Centre SPIN, Departement PEG, F - 42023 Saint-Etienne France

[‡]Multiphase Flow Research Center (NUEM), Federal University of Technology – Paraná (UTFPR), Rua Deputado Heitor Alencar Furtado, 5000, Bloco N, CEP 81280-340, Curitiba/PR, Brazil

[#]Phases to Flow Laboratory, Chemical and Biological Engineering Department, Colorado School of Mines, 1500 Illinois St., Golden, CO 80401, USA

Abstract. This study proposes a criterion for safe transportability of gas hydrate slurries in oil-dominant flowlines. Fluids chemistry plays a role on how the particles agglomerate, which occurs in the time window the particles take to decrease their porosity because of crystallization in the capillary walls or to seal the water within the pores by the action of chemical additives, then completely preventing any water in the outer surface of the particle and avoiding liquid bridge formation (agglomeration). Hydrodynamic aspects come from the lift vs buoyancy/weight forces that tend to suspend/settle the particles, as well as the collision and disruption rates of particles that play a role on the agglomeration process. The criterion is rather simple and shows the importance of the subcooling of crystallization, water cut, mixture velocity, and the oil-water interfacial tension that can be lowered by the use of additives. A simple chart for assuring safe, fully suspended slurry flow (low plugging risk) is proposed, called *slurry phase map*, and directives of its use for flowline design and management are discussed. Discussion is also given upon how to scale up laboratory measurements into field conditions by the proposal of a new dimensionless group, called *Bassani number*.

Keywords: flow assurance, gas hydrates, slurry, transportability, phase map.

1. Introduction

Gas hydrates are crystalline structures formed by hydrogen-bonded water molecules that entrap gas molecules in a clathrated network[1]. Water is nearly ubiquitous as a co-product in the production of gas and oil and if no strategy to avoid hydrate formation is implemented, the hydrate crystals form because of the typical high pressure and low temperature conditions in flowlines. The hydrate management strategy consists of letting hydrates form, but assuring their stable flow by preventing their agglomeration and accumulation along the flowline. That is, the particles need to flow suspended by the liquid phase, as homogeneously as possible, without significant accumulation or bedding, otherwise partial restrictions will occur, which considerably increase head losses[2] and can lead to plugging conditions in flowlines. If the slurry remains dispersed, then the production is assured as long as the hydrodynamics overcomes any increased friction coming from particle-fluid interactions, usually modeled through the concept of an apparent viscosity.

Literature presents several descriptions of apparent viscosity models coupled with multiphase flow hydrodynamics of hydrate slurries[3–7]. Those models however assume no partial restrictions, that is, that the slurry is always perfectly homogeneous and suspended; otherwise a transient multiphase flow framework with Lagrangian tracking of the particles is required[8,9], which is a substantially more complex problem. In these grounds, the missing key is a criterion that assures the stable slurry flow for a given set of production conditions, which is the purpose of this paper.

2. Slurry Hydrodynamics of Crystallizing Particles

Particles flow suspended inside of a liquid carrier phase whenever the lift forces overcome combined buoyancy and weight forces, as depicted in Figure 1(a). That is, for a given particle shape, size and concentration, and for a given particle-liquid density ratio, there is a critical velocity above which the particles are fully suspended under flow. This is the concept of *critical settling velocity*[10]. These phenomena are purely based on hydrodynamics, that is, occur in the particle size-scale and relate to the turbulent eddies of the flow in the same scale. Several studies relate the critical settling velocity of slurries with hydrodynamic variables[11–14].

Fluids chemistry however comes at play when dealing with gas hydrates[15]. Some new evidences reported in literature are discussed next and will be of great importance for the development of the criterion for stable slurry transportability. They concern the hypotheses that can be adopted for the level of mixture velocity in order to estimate the lift forces, and for the size and concentration of the

particles, as well as their evolution coming from the common crystallization processes of nucleation, growth, agglomeration, and breakage.

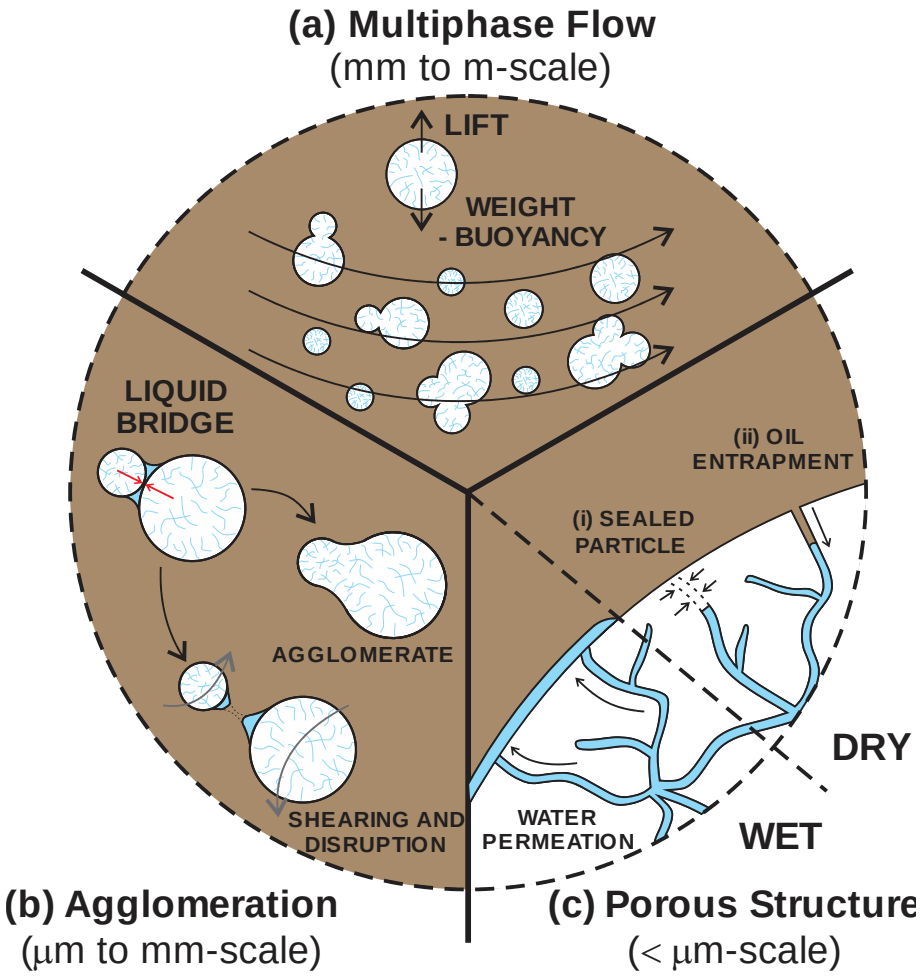

Figure 1. Depiction of the hydrodynamics of crystalizing gas hydrates particles. (a) Particles are suspended when the lift forces overcome the combined buoyancy and weight forces, and depend on the particle size and concentration. (b) The particle size increases because of agglomeration caused by binding forces coming from liquid bridges. (c) The liquid bridges are formed because of water permeation through the particle, with consequent water spreading over the outer surface of the particle. There are two ways to avoid water permeation and therefore to avoid the formation of wet particles that lead to agglomeration: (i) by sealing the water content inside the particle because of a fast crystallization in the capillary walls (high subcooling), or (ii) by promoting oil entrapment at the far end of the capillaries (use of additives).

Gas hydrate formation consumes gas, a phase of high specific volume, to form a solid, a phase with low specific volume. That is, the volume of mixture decreases considerably as the crystallization happens, causing the mixture to decelerate[3] and decreasing the lift forces that

suspend the particles. From recent simulations of hydrocarbon gases in oil-continuous systems[5], it was observed however that gas release because of frictional head losses causes the mixture to accelerate along the flowline, compensating any deceleration coming from hydrate formation. That is, the mixture velocity at the flowline inlet is the smaller one along the entire flowline and can therefore be adopted to estimate the lift forces of the particles. This hypothesis is valid when dealing with gases with high affinity with the continuous liquid phase, such as hydrocarbon gases in oil-continuous systems.

Still in oil-continuous scenarios, all free water is reported to rapidly get entrapped inside the porous structure of the particles during the onset and initial growth period of hydrate formation[15,16] because of the hydrophilic nature of gas hydrates[17]. This means that the initial concentration of particles can be considered the same as the water cut. The population of particles then evolves in time because of crystalline growth, agglomeration, and breakage. Growth is related to ~ 10% of particle volume variation because gas hydrates are slightly less dense than water[5], so growth can be discarded as an important contributor into the variation of the total volumetric fraction of particles. For example: if the system has 30 vol% water cut prior to the onset of hydrate formation and then all water is converted into hydrates, then the final volume content of gas hydrates will be ~ 33%. Furthermore, water conversion into hydrates can vary widely but it is often much lower than 50-60%[18–20], so this variation is even lower.

Agglomeration and breakage, in turn, will only relate to variations in the concentration of particles if water or oil is entrapped or released from the porous structure during these processes[15,21]. The oil entrapment can be of great importance, eventually causing a complete dry out of the system[22]. But its modeling is of a greater complexity and therefore usually neglected in literature. As a rule-of-thumb, the particle volumetric concentration can be approximated by the water cut of the system.

Another important aspect is the particle size. In oil-continuous systems, the favorable sites for gas hydrate formation are on the water droplet surface because the curved oil-water interface is energetically favorable and because the oil phase presents a much greater availability of gas[23], valid for hydrocarbon gases. Therefore, it is safe to assume that the initial particles sizes have the same size of the water droplets. Although the initial growth process is very fast, occurring in a few seconds[5], a quick rearrangement of the oil-water interfaces during the onset of formation can occur as well[24], leading to much larger initial particles than water droplets. This rearrangement is caused

by the perturbation of the interfacial energy once the first hydrate seeds nucleate in the oil-water interface, leading to a quick coalescence of water droplets while their water content is getting entrapped in the porous particles. Experimental evidence however point out that the initial particle size still remains in the same order of magnitude of the water droplets[16,21,25], in the 10-1000s micron-scale, and therefore droplet size models can be used as an estimative of the initial particle size. This is expected to hold for low water cuts and high flowrates, where the water droplets do not interact during the onset of formation – typical values of low water cut are of up to 10-20%, but the actual values depend on the fluid properties and flow conditions (i.e., flow regime). Several droplet size models exist and they capture the fact that the turbulent flow furnishes the necessary kinetic energy to disrupt the water-oil interfaces, thus sustaining the higher state of energy coming from the droplets surface creation[26–28].

The particles then increase in size. As already discussed, the increase coming from crystal growth is expected to cause at most a 10% variation, and can therefore be discarded. The more pronounced variations in size come from agglomeration and breakage. Breakage is difficult to evaluate[29], as it relates to fluid-structure interactions, where the flow shearing and/or any impact of collision causes the particles to split[15]. It is difficult not only to predict on how many debris the particle will split into and the relative size of the debris[29], as well as hydrate particles are porous with properties that evolve in time because of crystal ageing and transport-limited growth. Breakage can however be discarded by recognizing that the worst-case scenario is when particles only agglomerate, that is, this hypothesis is conservative in the point-of-view of industrial applications.

The agglomeration process, in turn, depends on the outer surface state of the particle[15,21,25]. Because in oil-continuous systems all water is entrapped inside the porous particles, and because hydrates are hydrophilic, then water tends to permeate through the particle and to spread over its outer surface[15], as presented in Figure 1(c). If this happens, then any particle collision leads to the formation of a liquid bridge[21], creating a binding (attractive) force related to the oil-water interfacial tension $\sigma_{o/w}$, Figure 1(b). The collided particles thus remain aggregated during a certain time-lapse that comes from the competition between the liquid bridge forces and the flow shearing[21,30]. Depending on the time-lapse the particles remain aggregated, the water content of the liquid bridge binding the aggregate can crystallize, forming an agglomerate[21,31]. The mechanical stability of the agglomerate is much higher than the one of the aggregate, coming from the yield stress of the crystal instead of the oil-water interfacial tension.

It was shown however that water can be prevented to permeate through the particles and to spread over the outer surface[16,25]. Because crystallization happens mainly in the capillary walls, then the particle porosity decreases in time, sealing the water content inside of the particle – see detail (i) of Figure 1(c). These are called *dry particles* and they are inert in the sense of agglomeration because they cannot form any liquid bridge upon collision. Because the porosity of the particle decreases in time, then a particle that is initially wet can dry out in time. Agglomeration only happens during the time window the particles are wet and, once they dry out, a stable, maximum agglomerate size is reached[21]. The particles not necessarily become dry when the porosity of the outer surface becomes zero, but when the permeation is slower than the crystal integration at the outer surface, thus all water arriving at the outer surface will instantly crystallize, avoiding a free water layer to form over the particle. The permeation rate, in turn, is inversely proportional to the particle porosity and to interfacial properties. Additives (e.g., anti-agglomerants) with surfactant properties induce a decrease in the interfacial tension of the oil/water interface, allowing oil to fill the pores, thus decreasing the permeation rate[25], or even completely blocking any water permeation if oil gets entrapped at the far end of the capillaries[15] – see detail (ii) of Figure 1(c).

Recently, we proposed an expression for the stable agglomerate size of hydrates in oil-continuous systems that consider the abovementioned phenomena[21]. In this article, we use this expression coupled with a droplet size model[28] for the initial crystal size, and with a critical settling velocity model[13] to predict if the slurry is transportable.

3. Criterion for Safe Transportability of Gas Hydrate Slurries in Oil-Dominant Systems

A hydrate slurry is said to be safe for production if it is transported fully suspended along the entire flowline, without any accumulation or bedding/settling – this is called a *stable slurry flow*. It occurs when the mixture velocity is equal or higher than the critical settling velocity of the slurry

$$J_{inlet} \geq J_{crit} \tag{1}$$

where the mixture velocity at the flowline inlet J_{inlet} is used as reference. Notice that, for safe transportability, hydrodynamics still needs to overcome any increased shear stresses (apparent viscosity) because of the presence of the particles (this aspect is outside the scope of this study).

Literature presents several models for critical settling velocity. For example, Oroskar and Turian's[11] study is one of the most complete, but their expression needs iterative solutions, which is

a downside when a simple criterion is sought. The correlation of Spells apud[14] is therefore assumed here – note that other correlations may be used as well, but the formalism would follow that described here. Some further simplifications are handled to this expression: (i) the particle density is assumed close to the water density because the particles are composed of water entrapped inside the hydrate porous medium[15], because hydrates and water have similar densities[32], and because water conversion into hydrates is commonly much less than 100%[18–20], and (ii) with the same assumption, the slurry density is estimated as $\rho_{slurry} \approx \rho_w \mathrm{WC} + \rho_o (1-\mathrm{WC})$, where WC is the water cut. Therefore, the critical settling velocity comes

$$J_{crit} = C_1 \left\{ g d_{p,\max} \left(\frac{\rho_w}{\rho_o} - 1 \right) \left(\frac{D}{\mu_o} \right)^m \left[\rho_w \mathrm{WC} + \rho_o (1-\mathrm{WC}) \right]^m \right\}^q \tag{2}$$

where $C_1 \approx 0.05$, $m \approx 0.775$ and $q \approx 0.816$ are the constants regressed by Spells apud[14], valid for slurry flow without an important concentration of particles over 1 mm (fine suspension). This model does not consider: (i) the induced turbulence of the gas phase into the liquid, such as the wake zone behind elongated bubbles occurring in slug flow pattern, which would tend to increase the critical settling velocity; nor (ii) the restriction one phase cause into the other, such as in stratified flow, with consequent deceleration of the liquid film because of close contact to the wall, which would tend to decrease the critical settling velocity. Furthermore, it should be noticed that the fitting of critical settling velocity correlations is usually done for sand and/or coal, that is, for solid-liquid density ratios much greater than unity, which is not representative of gas hydrates. In the future, these constants should be regressed against proper databases using particles that mimic the properties of gas hydrates[33]. In the absence of such, the model is used as a first approximation. The trends of those correlations are nevertheless expected to hold, because any settling model captures, to some extent, the physics behind the competition of lift vs buoyancy/weight forces, as well as the viscous effects that delay the settling period of the particles (more is discussed in section 1 of the Supporting Information).

As discussed in the last section, the missing key was the particle diameter, which evolves along the flowline because of agglomeration. Here, we adopt the model developed in a recent study of our group for the maximum agglomerate diameter[21]

$$d_{p,\max} = d_{p,in} + \frac{2k_7}{k_{fT}\Delta T} \sqrt{\frac{\rho_o f J_{inlet}^3}{\mu_o D}} \left[1 + \frac{k_6}{k_{fT}\Delta T} \frac{\rho_o}{\sigma_{o/w}} \frac{f J_{inlet}^3}{D} \right]^{-1} \max \left\{ 0 \; ; \; \ln \left[k_4 \sigma_{o/w} \cos\theta_{o/w/h} \frac{\zeta}{k_{fT}\Delta T} \right] \right\} \tag{3}$$

which happens when the particles dry out and stop furnishing the necessary water for liquid bridge formation. This depends: (i) on the shearing in the system, related to the mixture velocity J_{inlet}, to the flowline diameter D, and to the oil density ρ_o and viscosity μ_o; (ii) on the presence/use of additives, that cause the oil-water interfacial tension $\sigma_{o/w}$ to decrease; and (iii) on the subcooling ΔT for hydrate formation of the system, that acts on sealing the water inside the particle. The parameter ζ represents the interconnectivity of the porous medium, which decreases with the subcooling. It comes from the following fitted function

$$\zeta \approx \zeta_{\max} + \frac{\zeta_{\min} - \zeta_{\max}}{1 + \zeta_{\max} \exp\left[-a_6 \left(\Delta T - \Delta T^*\right)\right]} \tag{4}$$

where the constants regressed are $\zeta_{\min} \approx 0.001$, $\zeta_{\max} \approx 0.02$, $a_6 \approx 1\text{K}^{-1}$, $\Delta T^* \approx 15\,\text{K}$, $k_4 \approx 2\times10^{10}\ \text{m}^{-1}$, $k_6 \approx 2\times10^{7}$ m.Pa.s, $k_7 \approx 9.6\times10^{5}$ m.Pa.s and $k_{fT} \approx 5\times10^{5}$ Pa/K, retrieved from experiments for methane and for a gas mixture (92 mol% methane + 8 mol% propane), in oil-continuous systems, with 30% water cut, and an oil viscosity of 10 cP[5,21].

Eq (3) depends on the initial particle size, herein considered equal to the water droplet size before the onset of hydrate formation. The model of Brauner[28] is adopted

$$\frac{d_{p,in}}{D} = C_2 \text{We}_o^{-3/5} \text{Re}_o^{0.08} \left[\frac{\text{WC}}{1-\text{WC}}\right]^{3/5} \left[1 + \frac{\rho_w}{\rho_o}\frac{\text{WC}}{(1-\text{WC})}\right]^{-2/5} \tag{5}$$

where $\text{We}_o = \dfrac{\rho_o J_{inlet}^2 D}{\sigma_{o/w}}$ is the Weber number of the oil phase and $\text{Re}_o = \dfrac{\rho_o J_{inlet} D}{\mu_o}$ is the Reynolds number of the oil phase. The constant regressed by Brauner stays in the range of $5 \le C_2 \le 11.5$, and the expression is valid for $\text{Eo} = \dfrac{\left(\rho_w - \rho_o\right) g D^2}{8\sigma_{o/w}} > 5$ and $\dfrac{d_{p,in}}{D} < 0.1$. Eq (5) in the way presented here, with Weber and Reynolds numbers for the oil phase and using the water cut, is specific for oil-continuous systems. Notice however that Brauner's[28] expression is valid for water-continuous systems as well, as long as the oil cut and the Weber and Reynolds number of the water phase are used. Brauner[28] still suggests other relationships for $\text{Eo} < 5$ and $\dfrac{d_{p,in}}{D} > 0.1$, and for dilute dispersion as well, but the one shown in eq (5) is representative of the range of parameters tested in this study.

One shall now recognize that eqs (2) to (5) depend only on design parameters, such as the fluid and interfacial properties, the flowline geometry, the subcooling, and the hydrodynamic parameters such as water cut and mixture velocity at the flowline inlet. That is, for a given set of conditions and fluid properties, any engineer is able to evaluate the critical settling velocity of the slurry by simple substitution of values. From eq (1), this is the minimum velocity the engineer needs to assure at the flowline inlet in order to promote fully suspended hydrate slurries.

4. Slurry Phase Map for Oil-Dominant Systems

Figure 2 shows the evaluation of the criterion of eq (1), using the critical settling velocity, stable agglomerate size and droplet size models of eqs (2) to (5), for an 8 in-ID flowline considering an oil with 10 cP, 850 kg/m^3 and $\theta_{o/w/h} = 60^o$. A total of 1000 set of conditions were evaluated, randomly chosen inside $0.25 \le J_{inlet} \le 2$ m/s, $5 \le \mathrm{WC} \le 50\%$, $1 \le \Delta T \le 10$ K and $1 \le \sigma_{o/w} \le 5\times10^{-2}$ N/m. These parameters are considered to be representative of oil and gas production systems. The criterion is non-linear in several parameters, but a great influence of four parameters was observed: the mixture velocity J_{inlet} (evaluated at the flowline inlet), the water cut WC, the subcooling ΔT and the oil-water interfacial tension $\sigma_{o/w}$. By combining these parameters into the axes of the slurry phase map of Figure 2, two defined regions are found. The cases of stable slurry flow (fully suspended particles without accumulation or bedding) are plotted in green, and the unstable ones in red. The border in between safe and unsafe production of oil-dominant when gas hydrates form is well captured by a power scale

$$\frac{\Delta T}{\sigma_{o/w}\mathrm{WC}} = C_1 J_{inlet}^{m_1} \tag{6}$$

and is plotted by the dashed line of Figure 2. The values retrieved are $C_1 \approx 842$ and $m_1 \approx -3.35$ [SI units], but they depend on the flowline geometry and fluid properties. Sensitivity to the oil viscosity and to the flowline diameter is discussed in section 1 of the Supporting Information. Two general suggestions are: (i) that the correct values of these constants need further regression and testing against wider databases (preliminary tests are presented in section 2 of the Supporting Information) and (ii) that the engineer always needs to consider a safety factor over the prediction of the transition by, say, majoring the mixture velocity in at least 30%, as the transition is not a defined-line, but a region where transition is probable.

The slurry phase map captures the following aspects:

(i) Higher subcooling causes faster sealing of the particles, thus they take less time to dry out, ceasing the liquid bridge forces. This incurs in smaller stable agglomerate sizes, thus stable slurry flow conditions are easier to be reached.

(ii) By the presence/use of additives with surfactant properties, the oil-water interfacial tension is lowered, thus permeation of water through the porous particle is decreased, or the far end of the pores get filled with oil. This promotes smaller time-scales for the particles to dry out, leading to smaller agglomerates and promoting better suspension of the slurry. Furthermore, surfactant additives weaken the liquid bridge forces, thus decreasing the time-lapse for consolidation, which also contributes to form smaller agglomerates.

(iii) The higher the water cut, the higher the probability of collision between particles and the higher the initial particle size, leading to larger agglomerates that promotes settling of the slurry.

(iv) For a given stable agglomerate size, there is a minimum velocity of the mixture so that lift forces overcome combined buoyancy and weight, thus suspending the particles.

One should now recognize that, although the criterion of eq (6) is rather simple, all of the abovementioned trends are in agreement with simulation trends reported in our previous studies that use much more detailed physics and much more sophisticated mathematics[15,21,25]. Section 2 of the Supporting Information brings the comparison of the slurry phase map against Kakitani's[16] dataset using a rock-flow cell apparatus and shows a remarkable agreement considering that no direct fittings are done and that there is still room for a vast improvement in the experiments.

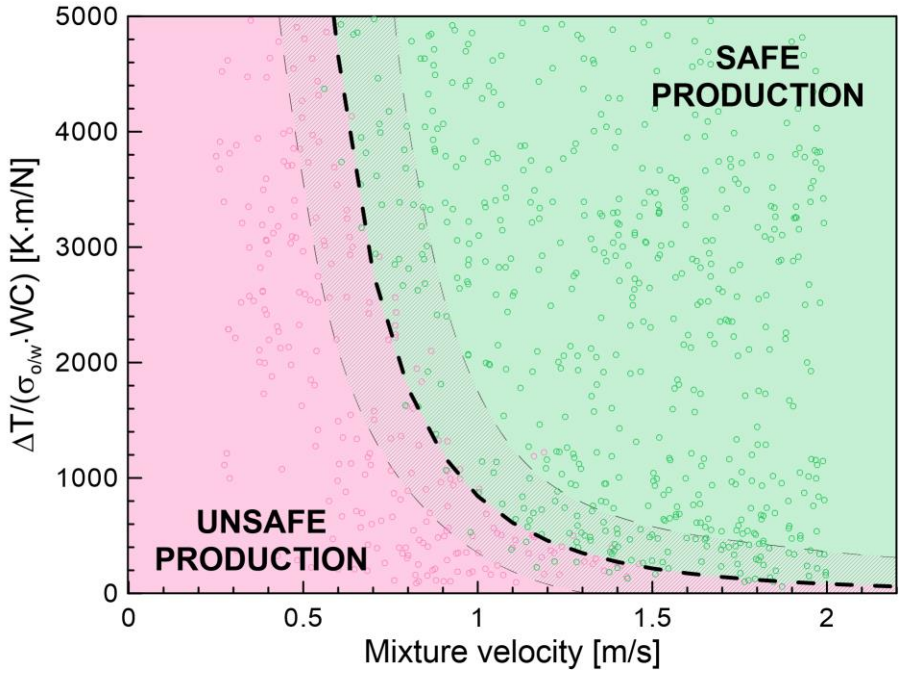

Figure 2. Hydrate slurry phase map for hydrate management. The dashed line is evaluated upon eq (6) and represents a region of transition from unstable to stable slurry flow. For demonstration, the data in the plot are evaluated upon criterion of eqs (1) to (5) for $D = 8\,\text{in}$, $\mu_o = 10\,\text{cP}$, $\rho_o = 850\,\text{kg/m}^3$ and $\theta_{o/w/h} = 60^o$ covering $0.25 \le J_{inlet} \le 2\,\text{m/s}$, $5 \le \text{WC} \le 50\%$, $1 \le \Delta T \le 10\,\text{K}$ and $1 \le \sigma_{o/w} \le 5\times10^{-2}\,\text{N/m}$. Notice that the dashed line is valid for the flowline geometry and fluid properties adopted, and that further testing is suggested prior to any field application.

5. Application of Slurry Phase Map for Flowline Design and Management

Flowline design is always intended to give the maximum mixture flowrate (or mixture velocity) possible, in order to maximize production (oil produced). This goes alongside with the criterion proposed in here, as the higher the mixture velocity, the easier to stabilize the slurry. Because the velocity is the higher possible one, then the flow assurance engineer will always be working with a nearly vertical line during the design process, as presented in Figure 3. This means that there is a commitment in the combined value of $\dfrac{\Delta T}{\sigma_{o/w}\text{WC}}$ in order to assure a fully suspended hydrate slurry. The water cut depends on the reservoir and varies with the life of the field, but for the first years of production it can be considered constant (water cut variations with time are addressed afterwards). Therefore, the variables that the engineer shall optimize are the subcooling and the oil-water interfacial tension.

In Figure 3, state A represents the velocity and water cut at the initial lifetime of the well, and no optimization was yet done in the subcooling and in the oil-water interfacial tension. The goal here is to achieve state B, that is, the deepest state possible inside the safe region, with slurries that are harder to settle down. Let us now understand how to optimize the subcooling and the oil-water interfacial tension.

The subcooling needs to be maximized in order that state A gets displaced upwardly towards state B. High subcooling causes the particles to quickly seal up, so liquid bridges will be minimized and agglomeration will be prevented. The subcooling for a given gas and a given system pressure depends on the use of thermodynamic inhibitors and on the thermal insulation of the flowline. In the chart of Figure 3, a higher subcooling means that state A will be displaced upwardly, towards state B'. The first conclusion here is that *no thermodynamic inhibitors should be injected when dealing with hydrate management*, otherwise the subcooling will be decreased because of a decreased equilibrium temperature of hydrate formation for the given system pressure.

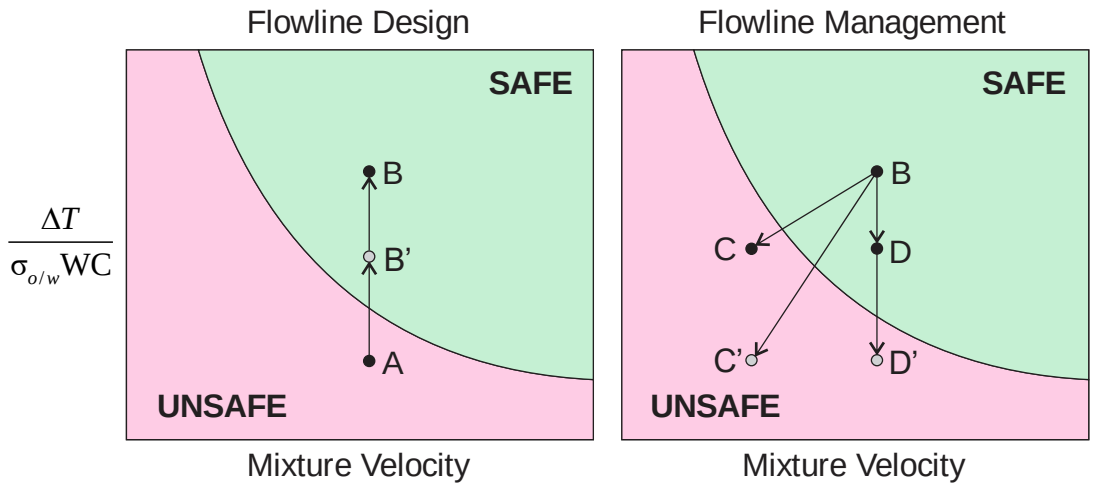

Figure 3. Use of the hydrate slurry phase map for flowline design and management. A: water cut and mixture velocity at the beginning of the lifetime of the well if nothing is done regarding hydrate management. B: Same as A, but subcooling was maximized by correct design of flowline insulation and by no use of thermodynamic inhibitors, and oil-water interfacial tension was minimized by insertion of additives. C': as the years pass, the mixture velocity decreases because of well depletion, and the water cut increases. C: same as C', but a more effective additive is employed. D': as the years pass, the water cut increases, but gas is re-injected into the well, sustaining the reservoir pressure and keeping a nearly constant mixture velocity. D: same as D', but a more effective additive is employed.

The second conclusion is that the *flowline insulation should ideally not be used, at least for hydrate management purposes*. The subcooling is dictated by the competition between the heat release during hydrate formation and the heat exchange with the external medium. The heavier the insulation, the higher the mixture reheat toward the equilibrium temperature during the onset of hydrate formation, causing the subcooling to decrease[5]. Of course that, prior to taking the insulation off, other flow assurance aspects need to be regarded. One potential issue that might arise is wax deposition. Another one, concerning gas hydrates, is the potential of migrating to a hydrate avoidance strategy at the end of the lifetime of the field, when the water cut achieves intermediary to high values, to be discussed latter in this section.

The second variable the flow assurance engineer can change is the oil-water interfacial tension, and it should be minimized in order to move state A upwardly. Crude oil with surface active compounds and effective AAs are reported to have surfactant properties, that is, to lower the oil-water interfacial tension. Therefore, depending on the strength and concentration of additives present/used, state A moves upwardly towards state B'. One should notice, however, that for a given type of additive, there is a limit in the additive concentration above which the oil-water interfacial tension is no longer lowered. This happens when all oil-water interfaces get saturated with the surfactant, and the introduction of more of the same will not have a meaningful influence. Of course that different multiphase flow patterns incur in different saturation dosages, and therefore a critical saturation value for one flowline is not expected to be the same that in another flowline, or when dealing with different oil properties, liquid loadings and/or water cuts. The definition of that saturation concentration is complex to be evaluated, but let us assume that the system saturation with additive is guaranteed by the engineer. In this case, it is important to keep in mind that the increase of injection of the same additive will have no impact in improving the stable slurry flow.

In that case, the flow assurance engineer should search for a stronger additive. In one hand, stronger surfactants can invert hydrates wettability into lipophilic, thus entrapping oil close to the outer surface of the particles and promoting dry particles that do not agglomerate, as already discussed from detail (ii) of Figure 1. However, if the oil entrapment is important (very strong additive), and especially when the system has strong shearing that promotes fine breakage of the hydrate particles, then the hydrate-oil-water forms a complex structure of non-Newtonian behavior that presents a cream aspect, see the videos of Chen et al.[34]. The non-Newtonian behavior incurs in

considerable increased head losses that are far more complex to deal with and often not considered by most hydrodynamic tools.

Finally, by combining both high subcoolings and the use of additives with surfactant properties, the flow assurance engineer can displace the production to the more stable state, state B of Figure 3. Of course that assuring the correct conditions of production inside the slurry phase map of Figure 3 is not the only requirement for safe production. One still needs to assure that the hydrodynamics always overcome any increased head losses coming from stresslets and/or collisions of the particles, usually done through an apparent viscosity model coupled to multiphase flow (out of scope in this paper).

Consider now that the flowline was designed to operate at state B of Figure 3, and the purpose now is to manage the production along the years. As time passes, the water cut increases and the mixture velocity (mixture flowrate) decreases. If nothing is done, then the system tends to state C'. That is, with the years, a flowline that was designed for a safe operation can start plugging. Before that happens, the engineer should lower the oil-water interfacial tension by changing the additive to a stronger one. Keep in mind here that the simple increase of additive concentration will probably not solve the problem, as the system might already have reached saturation. Another concern is not to choose an additive that is strong enough in order to promote non-Newtonian behaviors. If the engineer is able to do so, then instead of operating at state C', the production system would be operating at state C.

Another practice that is interesting to assure stable slurries for longer times is to re-inject gas or water into the well, so as to keep the reservoir pressure, thus sustaining a nearly constant mixture velocity over the years. The water cut, however, cannot be controlled, so the system moves from state B to state D'. Again, the engineer can change the additive as the years pass, then operating at state D.

Finally, one should be aware that once the water cut attains values where the system starts being water continuous, the free water content after the onset of hydrate formation can lead to hydrate deposition. The criterion proposed in this study is for oil-continuous systems only, and therefore deposits occurring in water-continuous systems are not captured. The suggestion here is that, once the flowline starts presenting higher water cuts and the continuous phase is water, the flow assurance engineer should change to a hydrate avoidance strategy by injecting thermodynamic

inhibitors. Several criteria for phase inversion are published in literature, and we suggest the one of Brauner and Ullmann[35].

Finally, the engineer shall keep in mind this potential migration from a hydrate management strategy to a hydrate avoidance strategy during the lifetime of the flowline, especially when designing the flowline insulation. The reason is that, whereas a heavy insulation is preferred for hydrate avoidance, no insulation at all should be used for hydrate management. The best commitment insulation-wise regarding hydrate avoidance and hydrate management should be carefully addressed by the flow assurance engineers.

6. Scaling Up Predictions into Field Conditions

We now turn the discussion to a practical concern of flow assurance engineers: *how to scale up laboratory data/models into field conditions?* Of course that the first challenge here is to find a suitable apparatus that controls velocity, such as a flow loop, but where visualization of the system morphology is accessible, such as a rock-flow cell. But even if that apparatus were to exist, it will never fully represent the shearing levels of the multiphase flow conditions of real fluids in the field, and therefore scaling up is a necessity. And for that purpose, one of the best options is the use of dimensionless groups.

In a previous study[21], we showed that the way to create a dimensionless number between the subcooling (in K), and the oil-water interfacial tension (in N/m), is through a modified Damköhler number, Da. In turn, by introducing density, viscosity, and flow diameter alongside the mixture velocity, one finds a Reynolds number, Re. Therefore, the criterion of eq (6) should be well represented by the following dimensionless form

$$\mathrm{Da} \approx C_2 \, \mathrm{Re}^{-m_2} \tag{7}$$

where the exponent $(-m_2)$ of the Reynolds number is here defined as negative because of the decaying trend shown in Figure 2. By transferring the Reynolds number to the left-hand side of the equation

$$C_3 \, \mathrm{Da} \, \mathrm{Re}^{m_2} \approx 1 \tag{8}$$

which represents the transition line of the slurry phase map of Figure 2 in a dimensionless form. We now need to recognize that a new dimensionless group can be defined upon the mixing of the

Damköhler number (crystallization) and the Reynolds number (hydrodynamics), which together represents the hydrodynamics of crystallizing particles

$$\mathrm{Ba} \approx C_3 \, \mathrm{Da} \, \mathrm{Re}^{m_2} \tag{9}$$

and if $\mathrm{Ba} > 1$, then the hydrate slurry remains fully suspended and production is safe. This new group was named *Bassani number* and stands for the combined chemistry- and hydrodynamic-aspects that lead to agglomeration of gas hydrate particles with their consequent settling in oil-dominant systems.

This dimensionless approach is not yet fully applicable in industry because: (i) the exact shapes of the Damköhler and Reynolds numbers (and therefore of the Bassani number) cannot be fully inferred with the current knowledge on multiphase flow induced-turbulence, crystal integration and porous medium closure values, and (ii) there is still a lack of wider experimental databases to stress out any proposed shape for the Bassani number and to propose the correct fittings. Next, we will give a recipe on how the Damköhler and Reynolds numbers can be inferred with the current knowledge in literature.

First, consider the evaluation of the Damköhler number, modified for gas hydrates. As defined in a previous study[21], this number represents the competition between crystal integration in the outer surface of the particle, and water permeation through the porous particle to its outer surface. If water permeation is faster, then $\mathrm{Da} < 1$, and a water layer forms over the particle (wet particles), leading to agglomeration. If the crystal integration is faster, then $\mathrm{Da} > 1$ and the water gets sealed inside of the porous particle and no water layer is formed around the particle (dry particle), thus preventing agglomeration.

There are two restrictions on fully evaluating the Damköhler number. The first is that it depends on closure parameters that are not fully understood in literature, such as the ones related to crystal integration and the porous medium. Here, we adopt reference values for methane hydrates. The second problem of evaluating the Damköhler number comes from the fact that the particle porosity decreases as gas hydrates keep forming. That is, the Damköhler number increases in time. To contour such, we evaluate the Damköhler number considering its initial value during the onset of hydrate formation, where the porosity is still high (close to 100%), and in this way the Damköhler number is fixed for a certain subcooling and oil-water interfacial tension. The time window for the Damköhler number to increase from its initial value up to unity is the same time window the particles have to agglomerate. In other words, the closer to unity the Damköhler number is during

the onset of hydrate formation, the smaller the maximum agglomerate size formed in the system. With these assumptions, the Damköhler number is evaluated as (see details on section 3 of the Supporting Information)

$$\mathrm{Da} \approx 1.5\times 10^{-4}\,\frac{\Delta T}{\sigma_{o/w}} \tag{10}$$

valid for methane hydrates. Notice that units are in SI, that is, ΔT is in [K] and $\sigma_{o/w}$ is in [N/m].

Next, consider the Reynolds number. The sole parameter that relates to the traditional definition of the Reynolds number in the form $\mathrm{Re} = \frac{\rho U D}{\mu}$ is the droplet size, eq (5). The critical settling velocity, in turn, depends mainly on two other dimensionless groups (see more in Poloski et al[13]): (i) the Froude number, that relates inertia to gravitational forces, and (ii) the Archimedes number, that relates gravitational forces to viscous ones. When multiplying the Froude and the Archimedes number, a modified Reynolds number appears, relating inertia to viscous forces, but it has not the same traditional shape often adopted in fluid mechanics. The same occurs for the maximum agglomerate size, eq (3), that relates to the shear rate of the flow, given by Kolmogorov theory as $\sqrt{\frac{\rho f U^3}{\mu D}}$. The shear rate, although not dimensionless, relates inertia to viscous forces, but again in a different way than the traditional Reynolds number. A further inconvenience yet arrives from the fact that these groups are defined for single-phase flow and therefore do not consider water cut and liquid loading, and any multiphase flow induced-turbulence effects (two-way coupled effects).

Here, we propose the use of a traditional Reynolds number in the form

$$\mathrm{Re} = \frac{\bar{\rho} J D}{\mu_o} \tag{11}$$

where

$$\bar{\rho} = \rho_w \mathrm{WC} + \rho_o \left(1 - \mathrm{WC}\right) \tag{12}$$

includes the water cut of the system and represents the density of the liquid phase.

Because this form of the Reynolds number does not fully capture all processes involved, correction factors are necessary for different oil viscosity and flowline diameter. As such, we propose the following expression for the Bassani number

$$\mathrm{Ba} = C\mathrm{Da}\left(\frac{\mathrm{Re}}{1000}\right)^{m}\left(\frac{\mu_o}{\mu_{ref}}\right)^{n}\left(\frac{D}{D_{ref}}\right)^{p} \tag{13}$$

and for $\mathrm{Ba} > 1$, the hydrate slurry remains fully suspended and the production is safe, valid for oil-dominant systems. The fitted values are $C = 0.01$, $m = 2.5$, $n = 3.5$ and $p = -4$, where the reference values for the correction factors are $\mu_{ref} = 0.01\,\mathrm{Pa.s}$ (equivalent to 10 cP) and $D_{ref} = 0.2032\,\mathrm{m}$ (equivalent to 8 in). The Damköhler number comes from eq (10) and the Reynolds number from eqs (11) and (12). Notice that *SI units shall always be used in this approach*. The fitting procedure was done over the theoretical model of eqs (1) to (5) covering 10k (ten thousand) points randomly evaluated inside the ranges of $\rho_o = 850\,\mathrm{kg/m^3}$, $\theta_{o/w/h} = 60^o$, $4 \le D \le 10\,\mathrm{in}$, $1 \le \mu_o \le 100\,\mathrm{cP}$, $0.1 \le J_{inlet} \le 5\,\mathrm{m/s}$, $5 \le \mathrm{WC} \le 50\%$, $1 \le \Delta T \le 10\,\mathrm{K}$ and $1 \le \sigma_{o/w} \le 5\times10^{-2}\,\mathrm{N/m}$, which are considered representative of oil and gas production scenarios. Details on the fitting procedure are given in section 3 of the Supporting Information. The critical value of the Bassani number over unity fails to predict fully suspended hydrate slurry flow for 0.05% only upon the evaluated cases. That demonstrates the powerfulness of the proposed Bassani number in transforming the slurry phase map into a dimensionless form. The range of $0.1 \le \mathrm{Ba} \le 1$ is a transition region where the slurry might be stable or not, and the Bassani number fails to predict 5.75% of the evaluated cases when inside this range. Details refer to Figure S4 of the Supporting Information. A general directive is *to always produce with the maximum Bassani number possible, and at least ensuring a safety factor over the value of unity*.

Finally, one important warning needs to be given. The fittings are theoretical and relate to the model and its intrinsic hypotheses, as discussed throughout this article. It is highly recommended to further test this new approach against wide databases before any actual application of this methodology. Possible improvements on the fittings and/or on the exact mathematical expression of the Bassani number may prove necessary in the future once wider databases are available.

7. Conclusions

This paper introduces a new methodology and tool for gas hydrate management: the slurry phase map. It consists of a graphical map in terms of primary engineering variables, namely the subcooling (driving force and influence of thermal insulation), the interfacial tension (presence/use

of additives), and the water cut and mixture velocity (which varies with the lifetime of the well). The slurry phase map presents a defined region of stable slurry flow of the gas hydrate particles, where agglomeration, settling/bedding or accumulation are minimized or negligible. The model is valid for oil-continuous systems, has theoretical grounds based on the physics of crystallizing particles under multiphase flow, and a preliminary comparison with experiments shows a remarkable agreement. The slurry phase map depends on the fluid properties and flowline geometry, and recipe is prescribed in order to retrieve the parameters needed prior to field application. Some guidelines on how this new tool can be used for both design and management of flowlines are given, as well as for its scaling-up for field conditions, giving rise to a new dimensionless group called Bassani number. The slurry phase map is an innovative and pioneer simple tool that has the potential to considerably change the way flow assurance engineers nowadays consider and implement gas hydrate management.

Supporting Information

The Supporting Information contains sensitivity results of the hydrate slurry phase map to the oil viscosity and flowline diameter, comparison of the slurry phase map against experimental results, and mathematic details on retrieving the expression for the Bassani number.

Corresponding Authors

*Amadeu K. Sum, asum@mines.edu

*Ana Cameirão, cameirao@emse.fr

*Rigoberto E.M. Morales, rmorales@utfpr.edu.br

Acknowledgements

The research groups are part of the Joint International Research Program on Gas Hydrates and Multiphase Flow (JIRP). The authors acknowledge the financial support of Région AURA Auvergne Rhône-Alpes through the project COOPERA FluEnergy, the Institut Mines-Télécom, the Coordination for the Improvement of Higher Education Personnel - Brazil (CAPES) - Finance Code 001, and TE/CENPES/PETROBRAS (5850.0103370.17.9).

Nomenclature

Roman letters

Ba	Bassani number	[-]
$d_{p,in}$	Particle diameter in the onset of hydrate formation	[m]
$d_{p,\max}$	Maximum, stable agglomerate diameter	[m]
D	Pipeline/rock-flow cell inner diameter	[m]
Da	Damköhler number	[-]
Eo	Eötvös number	[-]
f	Friction factor (Fanning)	[-]
g	Gravitational acceleration	[m/s^2]
J_{inlet}	Mixture superficial velocity (average velocity of the mixture as a whole), evaluated at the flowline inlet	[m/s]
J_{crit}	Critical settling velocity of the slurry (minimum velocity to assure full suspension of the particles)	[m/s]
Re	Reynolds number	[-]
ΔT	Subcooling	[K]
U	Velocity	[m/s]
We	Weber number	[-]
WC	Water cut	[-]

Greek letters

μ_o	Dynamic viscosity of the oil	[Pa.s]
$\theta_{o/w/h}$	Oil-water-hydrate wetted angle (water side), $\theta_{o/w/h} < 90^o$ (hydrophilic hydrates)	[rad]
ρ_o	Oil density	[kg/m^3]
ρ_w	Water density	[kg/m^3]
$\sigma_{o/w}$	Oil-water interfacial tension	[N/m]
ζ	Interconnectivity of porous medium	[-]

References

(1) Sum, A. K.; Koh, C. A.; Sloan, E. D. Clathrate Hydrates: From Laboratory Science to Engineering Practice. *Ind. Eng. Chem. Res.* **2009**, *48* (16), 7457–7465. https://doi.org/10.1021/ie900679m.

(2) Bassani, C. L.; Barbuto, F. A. A.; Sum, A. K.; Morales, R. E. M. Modeling the Effects of Hydrate Wall Deposition on Slug Flow Hydrodynamics and Heat Transfer. *Appl. Therm. Eng.* **2017**, *114*, 245–254. https://doi.org/10.1016/j.applthermaleng.2016.11.175.

(3) Bassani, C. L.; Barbuto, F. A. A.; Sum, A. K.; Morales, R. E. M. A Three-Phase Solid-Liquid-Gas Slug Flow Mechanistic Model Coupling Hydrate Dispersion Formation with Heat and Mass Transfer. *Chem. Eng. Sci.* **2018**, *178*, 222–237. https://doi.org/10.1016/j.ces.2017.12.034.

(4) Zerpa, L. E.; Sloan, E. D.; Sum, A. K.; Koh, C. A. Overview of CSMHyK: A Transient Hydrate Formation Model. *J. Pet. Sci. Eng.* **2012**, *98–99*, 122–129. https://doi.org/10.1016/J.PETROL.2012.08.017.

(5) Bassani, C. L. A Multiscale Approach for Gas Hydrates Considering Structure, Growth Kinetics, Agglomeration and Transportability under Multiphase Flow Conditions. PhD Thesis, Federal University of Technology - Paraná in collaboration with Mines Saint-Etienne, 2020.

(6) Zerpa, L. E.; Rao, I.; Aman, Z. M.; Danielson, T. J.; Koh, C. A.; Sloan, E. D.; Sum, A. K. Multiphase Flow Modeling of Gas Hydrates with a Simple Hydrodynamic Slug Flow Model. *Chem. Eng. Sci.* **2013**, *99*, 298–304. https://doi.org/10.1016/j.ces.2013.06.016.

(7) Shi, G.; Song, S.; Shi, B.; Gong, J.; Chen, D. A New Transient Model for Hydrate Slurry Flow in Oil-Dominated Flowlines. *J. Pet. Sci. Eng.* **2021**, *196*, 108003. https://doi.org/10.1016/j.petrol.2020.108003.

(8) Balakin, B. V; Hoffmann, A. C.; Kosinski, P. Experimental Study and Computational Fluid Dynamics Modeling of Deposition of Hydrate Particles in a Pipeline with Turbulent Water Flow. *Chem. Eng. Sci.* **2011**, *66* (4), 755–765. https://doi.org/10.1016/j.ces.2010.11.034.

(9) Balakin, B. V.; Lo, S.; Kosinski, P.; Hoffmann, A. C. Modelling Agglomeration and Deposition of Gas Hydrates in Industrial Pipelines with Combined CFD-PBM Technique. *Chem. Eng. Sci.* **2016**, *153*, 45–57. https://doi.org/10.1016/j.ces.2016.07.010.

(10) Peker, S.; Helvaci, S. *Solid-Liquid Two-Phase Flow*, 1st ed.; Elsevier Science: Amsterdam, 2007, 534 p.

(11) Oroskar, A. R.; Turian, R. M. The Critical Velocity in Pipeline Flow of Slurries. *AIChE J.* **1980**, *26* (4), 550–558. https://doi.org/10.1002/aic.690260405.

(12) Gillies, R. G.; Shook, C. A. Deposition Velocity Correlation for Water Slurries. *Can. J. Chem. Eng.* **1991**, *69* (5), 1225–1227. https://doi.org/10.1002/cjce.5450690525.

(13) Poloski, A. P.; Etchells, A. W.; Chun, J.; Adkins, H. E.; Casella, A. M.; Minette, M. J.; Yokuda, S. T. A Pipeline Transport Correlation for Slurries with Small but Dense Particles. *Can. J. Chem. Eng.* **2010**, *88* (2), 182–189. https://doi.org/10.1002/cjce.20260.

(14) Turian, R. M.; Yuan, T.-F. Flow of Slurries in Pipelines. *AIChE J.* **1977**, *23* (3), 232–243. https://doi.org/10.1002/aic.690230305.

(15) Bassani, C. L.; Melchuna, A. M.; Cameirão, A.; Herri, J.-M.; Morales, R. E. M.; Sum, A. K. A Multiscale Approach for Gas Hydrates Considering Structure, Agglomeration, and

Transportability under Multiphase Flow Conditions: I. Phenomenological Model. *Ind. Eng. Chem. Res.* **2019**, *58* (31), 14446–14461. https://doi.org/10.1021/acs.iecr.9b01841.
(16) Kakitani, C. Experimental Study of the Gas Hydrate Formation upon Shut-in and Restart of Gas and Oil Pipelines (in Portuguese), PhD Thesis, Federal University of Technology - Paraná, Curitiba, Brazil, 2019.
(17) Hirata, A.; Mori, Y. H. How Liquids Wet Clathrate Hydrates: Some Macroscopic Observations. *Chem. Eng. Sci.* **1998**, *53* (14), 2641–2643. https://doi.org/10.1016/S0009-2509(98)00078-5.
(18) Melchuna, A.; Cameirao, A.; Herri, J. M.; Glenat, P. Topological Modeling of Methane Hydrate Crystallization from Low to High Water Cut Emulsion Systems. *Fluid Phase Equilib.* **2016**, *413*, 158–169. https://doi.org/10.1016/j.fluid.2015.11.023.
(19) Kakitani, C. Study of Phase Equilibrium of Methane Hydrate and Mixture of Methane and Carbon Dioxide Hydrate (in Portuguese), MSc Thesis, Federal University of Technology - Paraná, Curitiba, Brazil, 2014.
(20) Straume, E. O. Study of Gas Hydrate Formation and Wall Deposition under Multiphase Flow Conditions, PhD Thesis, Federal University of Technology - Paraná, Curitiba, Brazil, 2017.
(21) Bassani, C. L.; Kakitani, C.; Herri, J.-M.; Sum, A. K.; Morales, R. E. M.; Cameirão, A. A Multiscale Approach for Gas Hydrates Considering Structure, Agglomeration, and Transportability under Multiphase Flow Conditions: III. Agglomeration Model. *Ind. Eng. Chem. Res.* **2020**, *59* (34), 15357–15377. https://doi.org/10.1021/acs.iecr.0c02633.
(22) Melchuna, A. M.; Glenat, P.; Rivero, M.; Sum, A. K. Measurements of Dispersant Additive on Hydrate/Ice Slurry Transport. In *11th North American Conference on Multiphase Production Technology*; BHR Group: Banff, Canada, 2018; p BHR-2018-143.
(23) Kashchiev, D.; Firoozabadi, A. Nucleation of Gas Hydrates. *J. Cryst. Growth* **2002**, *243* (3–4), 476–489. https://doi.org/10.1016/S0022-0248(02)01576-2.
(24) Song, G.; Li, Y.; Sum, A. K. Characterization of the Coupling between Gas Hydrate Formation and Multiphase Flow Conditions. *J. Nat. Gas Sci. Eng.* **2020**, *83*, 103567. https://doi.org/https://doi.org/10.1016/j.jngse.2020.103567.
(25) Bassani, C. L.; Sum, A. K.; Herri, J.-M.; Morales, R. E. M.; Cameirão, A. A Multiscale Approach for Gas Hydrates Considering Structure, Agglomeration, and Transportability under Multiphase Flow Conditions: II. Growth Kinetic Model. *Ind. Eng. Chem. Res.* **2020**, *59* (5), 2123–2144. https://doi.org/10.1021/acs.iecr.9b04245.
(26) Hinze, J. O. Fundamentals of the Hydrodynamic Mechanism of Splitting in Dispersion Processes. *AIChE J.* **1955**, *1* (3), 289–295. https://doi.org/10.1002/aic.690010303.
(27) Hughmark, G. A. Drop Breakup in Turbulent Pipe Flow. *AIChE J.* **1971**, *17* (4), 1000. https://doi.org/10.1002/aic.690170440.
(28) Brauner, N. The Prediction of Dispersed Flows Boundaries in Liquid-Liquid and Gas-Liquid Systems. *Int. J. Multiph. Flow* **2001**, *27* (5), 885–910. https://doi.org/10.1016/S0301-9322(00)00056-2.
(29) Herri, J. M.; Pic, J. S.; Gruy, F.; Cournil, M. Methane Hydrate Crystallization Mechanism from In-Situ Particle Sizing. *AIChE J.* **1999**, *45* (3), 590–602. https://doi.org/10.1002/aic.690450316.
(30) Balakin, B. V; Kutsenko, K. V; Lavrukhin, A. A.; Kosinski, P. The Collision Efficiency of Liquid Bridge Agglomeration. *Chem. Eng. Sci.* **2015**, *137*, 590–600. https://doi.org/10.1016/j.ces.2015.07.002.
(31) David, R.; Marchal, P.; Klein, J.-P.; Villermaux, J. Crystallization and Precipitation

Engineering—III. A Discrete Formulation of the Agglomeration Rate of Crystals in a Crystallization Process. *Chem. Eng. Sci.* **1991**, *46* (1), 205–213. https://doi.org/https://doi.org/10.1016/0009-2509(91)80130-Q.

(32) Sloan, E. D.; Koh, C. A. *Clathrate Hydrates of Natural Gases*, 3rd ed.; Taylor & Francis Group: Boca Raton, 2008, 734 p.

(33) Rosas, L. M.; Bassani, C. L.; Alves, R. F.; Schneider, F. A.; M.A., M. N.; Morales, R. E. M.; Sum, A. K. Measurements of Horizontal Three-phase Solid-liquid-gas Slug Flow: Influence of Hydrate-like Particles on Hydrodynamics. *AIChE J.* **2018**, *64*, 2864–2880. https://doi.org/10.1002/aic.16148.

(34) Chen, J.; Yan, K.-L.; Chen, G.-J.; Sun, C.-Y.; Liu, B.; Ren, N.; Shen, D.-J.; Niu, M.; Lv, Y.-N.; Li, N.; Sum, A. K. Insights into the Formation Mechanism of Hydrate Plugging in Pipelines. *Chem. Eng. Sci.* **2015**, *122*, 284–290. https://doi.org/10.1016/j.ces.2014.09.039.

(35) Brauner, N.; Ullmann, A. Modeling of Phase Inversion Phenomenon in Two-Phase Pipe Flows. *Int. J. Multiph. Flow* **2002**, *28* (7), 1177–1204. https://doi.org/10.1016/S0301-9322(02)00017-4.

Supporting Information of

Defining a Slurry Phase Map for Gas Hydrate Management in Multiphase Flow Systems

Carlos L. Bassani[†,‡], *Jean-Michel Herri*[†], *Ana Cameirão*[†*], *Rigoberto E.M. Morales*[‡*], *Amadeu K. Sum*[#*]

[†]Mines Saint-Etienne, Univ Lyon, CNRS, UMR 5307 LGF, Centre SPIN, Departement PEG, F - 42023 Saint-Etienne France

[‡]Multiphase Flow Research Center (NUEM), Federal University of Technology – Paraná (UTFPR), Rua Deputado Heitor Alencar Furtado, 5000, Bloco N, CEP 81280-340, Curitiba/PR, Brazil

[#]Phases to Flow Laboratory, Chemical and Biological Engineering Department, Colorado School of Mines, 1500 Illinois St., Golden, CO 80401, USA

1. Sensitivity of Slurry Phase Map to Flowline Diameter and Oil Viscosity

The slurry phase map presented by Figure 2 of the article is valid for a given flowline geometry and fluid properties. In this section, discussion is given on how the slurry phase map behaves for different flowline diameters and oil viscosities.

Figure S1(a) presents the sensitivity of the slurry phase map – that is, the transition line to stable slurry flow – to the flowline diameter. *Larger diameters cause the transition of the slurry phase map to shift to the right, thus decreasing the stable slurry region*. At a first glance, that might look counter-intuitive, because smaller diameters are easier to plug. To interpret the results, the variable we will be looking at is the shear rate, which is a combination between velocity, oil viscosity and flowline diameter[1]

$$\dot{\gamma} \approx \sqrt{\frac{2\rho_o f J_{inlet}^3}{\mu_o D}} \propto D^{-1/2} \tag{S1}$$

The shear rate is proportional to the local agitation of the turbulent velocity field, at the hydrate particle scale (10 to 1000 of microns), and is responsible for: (i) the lift forces that suspend the slurry and that play a role into decreasing the critical settling velocity, eq (2) of the article; (ii) the collision rate between particles and disruption rate of aggregated particles that are held together by a liquid bridge[1], that play a role into the stable agglomerate size, eq (3); and (iii) the splitting of the water droplets into smaller ones[2] prior to the onset of hydrate formation, that plays a role on the initial hydrate particle size, eq (5). Larger diameters incur in smaller shear rates, thus the initial particle size and the agglomeration rate are higher, and the lift forces are smaller (that is, the critical settling velocity is higher). These combined effects incur in the shifting of the slurry phase map to the right for larger diameters.

Figure S1(b) presents the sensitivity of the slurry phase map to the oil viscosity. *More viscous oils shift the transition to the left, increasing the region of stable slurry flow.* From eq (S1), a more viscous oil incurs in smaller shear rates, thus the influence of the oil viscosity is not coming from the aforementioned aspects (i) to (iii). The major role of oil viscosity is not in the shear rate, but on the viscous force that acts counter wise to the settling of the particle, perpendicularly to the flow direction, as depicted in Figure S2. Considering that this perpendicular settling velocity is much smaller than the flow velocity, one can use Stokes law

$$v_{settling} \approx \frac{g d_p^2}{18} \frac{\left(\rho_h - \rho_o\right)}{\mu_o} \propto \mu_o^{-1} \tag{S2}$$

This expression does not take into consideration the lift force coming from the turbulent field, which is far too complex to be introduced in such a simple expression. The Stokes law nevertheless shows that the settling velocity is inversely proportional to the oil viscosity. This explains why it is easier to promote particle suspension in viscous oils, that is, why the slurry phase map is shifted to the left for increasing viscosities.

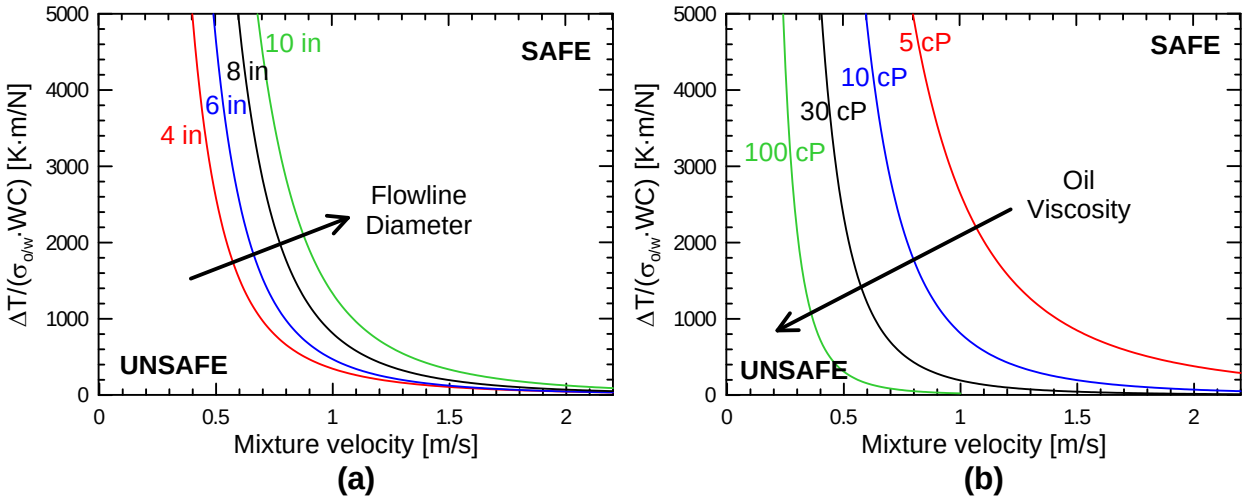

Figure S1. Sensitivity of slurry phase map to (a) the flowline diameter (for a 10 cP oil) and (b) to the oil viscosity (for an 8 in-ID flowline).

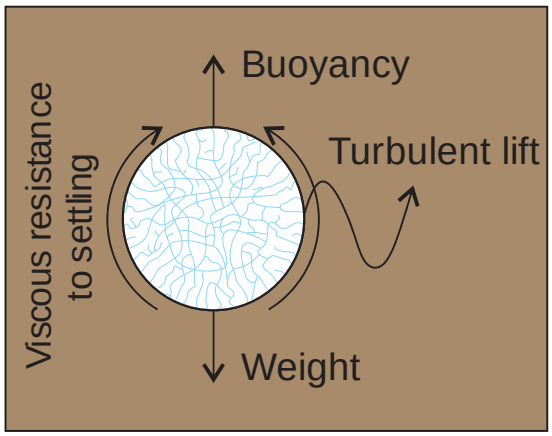

Figure S2. Simplified depiction of lift, weight, buoyancy and viscous forces acting perpendicularly to the flow direction, which competition defines the settling or suspension of the particles/agglomerates.

In an attempt of unifying parameters C_1 and m_1 of eq (6) of the article (transition to stable slurry flow) for different flowline diameters and oil viscosities, we propose the following fitted functions over the theoretical slurry phase maps of Figure S1

$$C_1 \approx 13.7 D \mu_o^{-1.3} \tag{S3}$$

$$m_1 \approx -8.7 D \mu_o^{0.14} - 2.43 \tag{S4}$$

where the diameter is in [m] and the oil viscosity in [Pa.s]. This functions comes from extended results of the theoretical method described in the article to generate the slurry phase maps, and thus should be further tested against larger databases prior to industrial application. The fittings were held for $4 \leq D \leq 10$ in and $5 \leq \mu_o \leq 100$cP. The fitted function for C_1 presents a deviation of ±30% against its theoretical value, whereas m_1 presents a deviation of ±15%.

2. Comparison of Slurry Phase Map with Rock-Flow Cell Experiments

In this section, we compared the theoretical slurry phase map proposed in the article against Kakitani's[3] dataset. She presents 18 experimental points for oil-dominant systems in a 50.8 mm-ID rock-flow cell apparatus, varying the rotational speed from 6 to 16 rpm (mixture velocity estimated in the range of 0.1 to 0.26 m/s[1]), the subcooling from 7.5 to 18 K, and the water cut from 10 to 30%. The liquid loading was kept constant at 50%, and tests were done with and without chemical additives. Additives were considered to decrease the oil-water interfacial tension in approximately 25% relatively to the general order of magnitude of $\sim 5 \times 10^{-2}$ N/m[1], but interfacial properties were not experimentally characterized. It should be noticed that Kakitani[3] classifies the flow as stable when a slurry is formed after particle breakage (or attrition) in the time-scale of 3 to 4 h. Here, the approach is more conservative, and if the system does not quickly converge to a dispersed state in the first 5 min after the onset of hydrate formation, then the system is considered not safe for production.

Figure S3 presents the slurry phase map for Kakitani's system. The black dashed line of Figure S3 represents the theoretical transition to stable slurry flow predicted by the method proposed in the article, with $C_1 = 65.2$ and $m_1 = -3.3$ [SI units]. The transition is displaced to the right when compared to the experimental dataset. A pure fitting of the experiments give the gray dashed line, where $C_1 = 60$ and $m_1 = -2.5$. This is a remarkable result given that: (i) the model have theoretical grounds based on population balance and mass transfer occurring at the porous scale[1,4,5], where several hypothesis were done regarding the geometry of the porous structure and agglomerates, as well as for the particle interaction with the turbulent flow field; and (ii) the experiments can still be enhanced by better predictions of the velocity field (or local shear rate), as well by better characterization of fluid and interfacial properties at high pressure. The theoretical results capture the behavior of the transition (the power law) and still predict the order of magnitude where it happens.

With improved experimentation, there is room for a vast improvement of parameters C_1 and m_1 in a near future. For instance, it is highly advised to not apply the criterion in industry prior to further testing and refining the values of C_1 and m_1.

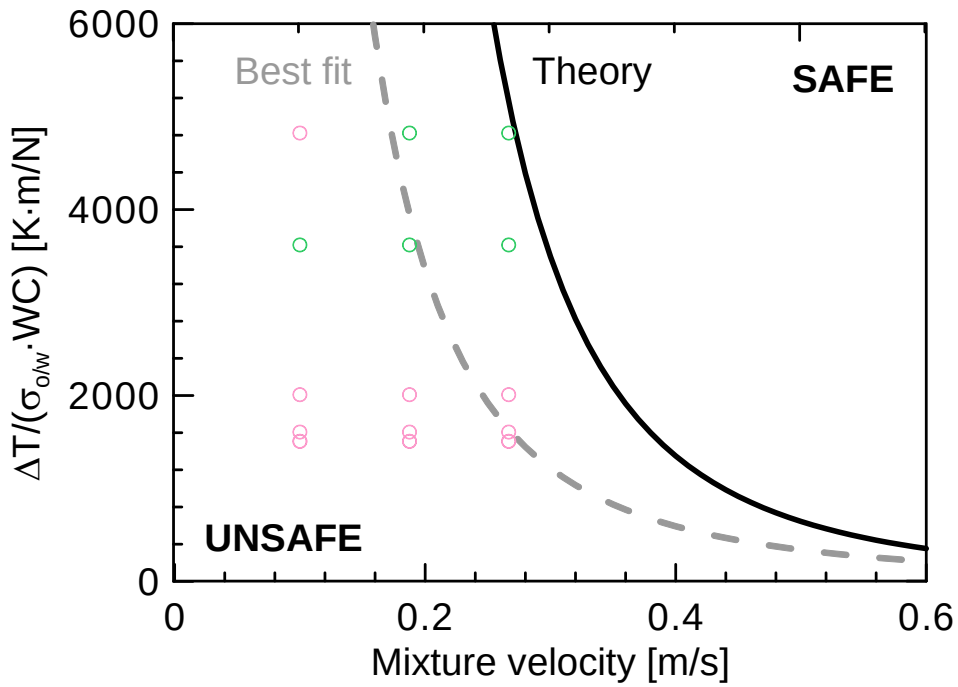

Figure S3. Slurry phase map of Kakitani's[3] dataset for a diameter of 50.8 mm and oil viscosity of 10 cP. The green dots are experimental results with stable slurry flow, and the red ones present considerable agglomeration and settling. The black line represents the theoretical transition to stable slurry flow coming from eq (6) of the article, with $C_1 = 65.2$ and $m_1 = -3.3$ [SI units]. The gray dashed line is the transition to stable slurry flow coming from a direct fitting of eq (6) with the experimental dataset, where $C_1 = 60$ and $m_1 = -2.5$.

3. Proposal of Expression for Bassani Number

Some choices are necessary to propose an expression for the new dimensionless group proposed at section 6 of the article, called Bassani number. Furthermore, because of restrictions on experimental data availability – the current available dataset that suits this work is the one of Kakitani's[3] which is composed of 18 experimental points only – then the fitting is over theoretical results. The choices made are discussed in this section.

The modified Damköhler number for gas hydrates was proposed in eq (42) of a previous study[5], and by substituting the permeation and crystal integration laws, one finds the following expression – notice that eq (43) of Bassani et al[5] is the inverse of the Damköhler number, Da^{-1}

$$\mathrm{Da} = 12\left(\frac{\mu_w M_w}{\rho_w}\right)\left(\frac{\tau^2}{\zeta \varepsilon r_c}\right)\frac{\eta r_p k_i k_{fT}}{\cos\theta_{o/w/h}}\frac{\Delta T}{\sigma_{o/w}} \tag{S5}$$

Several parameters in this expression are not fully defined in literature. The approach here is to consider the order of magnitude of reported values that hold for methane hydrates at common

measurement conditions, thus making the Damköhler number to depend on the subcooling and oil-water interfacial tension only. The water properties are well defined, where $\rho_w = 1000\,\text{kg/m}^3$ is the water density, $\mu_w = 1\times10^{-3}$ Pa.s is the water viscosity, and $M_w = 18\times10^{-3}$ kg/mol is the molar mass of water. The hydration number of $\eta \approx 6$ is a commonly adopted value for methane hydrates in literature. The porous medium parameters are not well defined, but here we adopt their order of magnitude, were $r_c = 0.5\times10^{-6}$ m is the capillary radius, $\tau = 5$ is the capillary tortuosity, $\zeta = 0.02$ is the capillary interconnectivity. Details on the range of values of these parameters are referred to Table 1 of Bassani et al[5]. The Damköhler number evolves in time as hydrates keep forming and as the particle porosity decreases. We therefore evaluate the Damköhler number during the onset of hydrate formation, where the porosity is still high, here considered as $\varepsilon = 0.9$. The particle size is considered as $r_p = 0.001\,\text{m}$ (in the order of magnitude of the millimeter). Parameter $k_{fT} = 5\times10^5$ Pa/K represents the transformation of fugacity driving force into subcooling and holds for methane at ~ 70 bar for subcoolings around 7 K, refer to Table 4 of Bassani et al[1]. The oil-water-hydrate wetted angle (water side), although dependent on the use of additives, is considered constant and close to $\theta_{o/w/h} = 60^o$ (hydrophilic hydrates, no wettability inversion coming from additives). Finally, the most sensitive parameter of the Damköhler number is the constant of proportionality of the crystal integration law (fugacity-based, first order), herein fixed as $k_i = 4.1\times10^{-11}$ mol/(m^{2}sPa) in conformity with our previous works[1,5]. A compilation of values of k_i can be found at Table A.1 of Bassani[6]. From the mentioned values, the Damköhler number comes

$$\text{Da} \approx 1.5\times10^{-4}\,\frac{\Delta T}{\sigma_{o/w}} \quad \text{for methane hydrates} \tag{S6}$$

where the subcooling, in [K], and the oil-water interfacial tension, in [N/m], are in the SI unit system. Notice that several considerations could be made differently, leading to other constants of proportionality. Only with more detailed experimentations one will be able to get a more accurate Damköhler number. Nevertheless, for the purposes of this study, the fact that the Damköhler number is proportional to the subcooling and inversely proportional to the oil-water interfacial tension brings the information on crystal integration at the outer surface of the particle, and on water permeation through the porous particle, which together relates to the physics of the particle being wet or dry. In other words, although the constant of proportionality might not be correct, the trends captured by the analysis to follow are expected to hold.

For the shape of the Reynolds number, and as discussed in section 6 of the article, there are different ways to relate inertia (the phenomenon that drives the motion) to viscous effects (the phenomenon that resists to motion). Those relate to the lift forces acting at suspending the slurry, to the shearing acting at the collision and disruption rates during agglomeration, and to the turbulent energy acting at disrupting the oil-water interfaces and promoting different water droplet sizes. The choice made was to use a traditional Reynolds number, eq (11) of the article,

based on the average liquid density, eq (12) of the article, which is a manner to include water cut effects. Notice that, by considering that hydrates have a density that is similar to water and that the particles are very porous and therefore mainly formed of water, then the density as defined in eq (12) of the article actually represents the density of the slurry.

From the choice of this shape of Reynolds number, one however cannot get rid of the dependency of the transition of the slurry phase map on the diameter and oil viscosity, as mentioned in Figure S1. The sole way to define a Bassani number that has a nearly constant critical value above which all systems are safe for production (stable slurry flow), independently on the geometry and fluid properties, is by further introducing degrees of freedom. This is made through dimensionless multipliers in terms of the oil viscosity, $(\mu_o / \mu_{o,ref})$, and the flowline diameter, (D / D_{ref}), where $\mu_o = 0.01$ Pa.s and $D_{ref} = 0.2032$ m are the adopted as reference values. Notice that the choice of the reference values is arbitrary, but the fittings will change if another reference value is chosen. The expression for the Bassani number then comes

$$\mathrm{Ba} = C\mathrm{Da}\left(\frac{\mathrm{Re}}{1000}\right)^m \left(\frac{\mu_o}{\mu_{ref}}\right)^n \left(\frac{D}{D_{ref}}\right)^p \tag{S7}$$

where the Reynolds number is divided by 1000 in order to avoid large values because of the exponent m.

Because of unavailability of experimental data, then the theoretical model of section 3 of the article, that is, eqs (1) to (5), are used to generate the values to fit eq (S7). In the future, these fittings shall be retrieved from experimental databases, once they are made available, but the fitting recipe will be the same. We generated 10k (ten thousand) results covering $\rho_o = 850$ kg/m^3, $\theta_{o/w/h} = 60^o$, $4 \le D \le 10$ in, $1 \le \mu_o \le 100$ cP, $0.1 \le J_{inlet} \le 5$ m/s, $5 \le \mathrm{WC} \le 50\%$, $1 \le \Delta T \le 10$ K and $1\times10^{-2} \le \sigma_{o/w} \le 5\times10^{-2}$ N/m. When the inlet velocity of the system is higher than the critical settling velocity of the slurry, $J_{inlet} > J_{crit}$, the system is classified as safe for production (stable slurry flow) and is plotted in green. Otherwise, it is plotted in red.

Figure S4 presents a plot of the Bassani number for all evaluated cases. The fitting of m, n and p is done to find a transition in between red and green cases that is nearly horizontal. We already know from the slurry phase map shown in Figure 2 of the article, and from the discussions over Figure S1 and Figure S3, that the exponent of the Reynolds number is $m \approx 2.5 - 3.5$. Notice that $m > 0$ (m is positive) because of the inversion of sign in the passage of eq (7) to (8) in the article. Furthermore, we know from Figure S1 that larger oil viscosities cause the stable slurry flow zone to increase, therefore $n > 0$ (n is positive); and that larger flowline diameters cause the stable slurry flow zone to shrink, thus $p < 0$ (p is negative). With these restrictions in mind, one is able to find a horizontal transition line in Figure S4 by adopting $m = 2.5$, $n = 3.5$ and $p = -4$. Finally, the constant $C = 0.01$ is fitted in order to centralize the transition line at a critical value of $\mathrm{Ba}_{crit} = 1$. *We emphasize once more that the fittings done comply with the theoretical approach*

of this article, but they shall be further tested and stressed out against wide experimental databases prior to any field application.

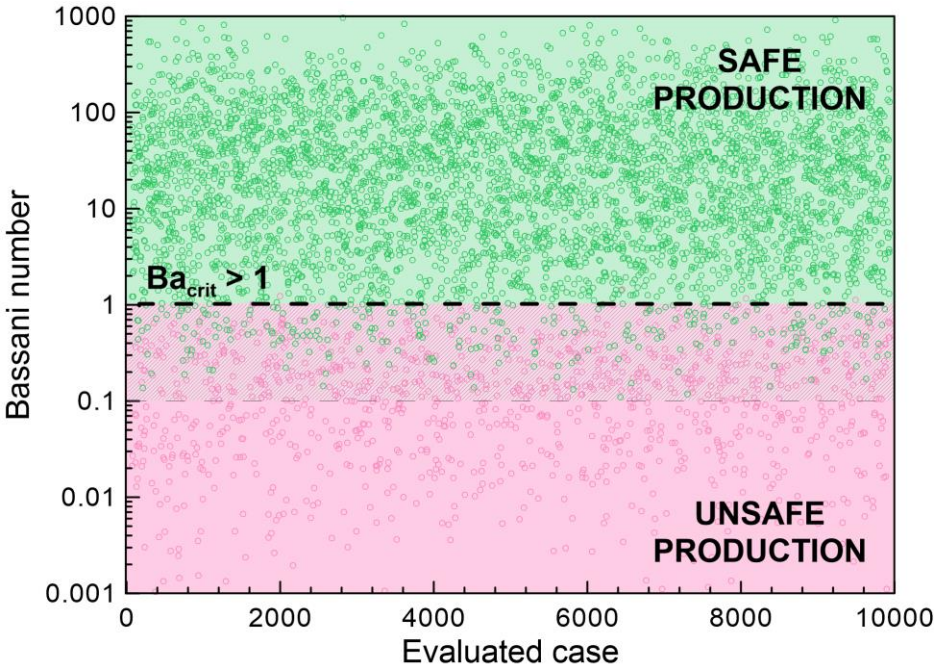

Figure S4. Bassani number evaluated from eq (S7) for 10k (ten thousand) points covering $\rho_o = 850\ \text{kg/m}^3$, $\theta_{o/w/h} = 60^o$, $4 \le D \le 10\ \text{in}$, $1 \le \mu_o \le 100\ \text{cP}$, $0.1 \le J_{inlet} \le 5\ \text{m/s}$, $5 \le \text{WC} \le 50\%$, $1 \le \Delta T \le 10\ \text{K}$ and $1\times10^{-2} \le \sigma_{o/w} \le 5\times10^{-2}\ \text{N/m}$. Green points represent stable slurry flow that is safe for production, whereas red points represent slurries that tend to settled down, causing accumulation and restrictions that are unsafe for production. This plot shows that systems with $\text{Ba} > 1$ are safe for production.

Additional References

(1) Bassani, C. L.; Kakitani, C.; Herri, J.-M.; Sum, A. K.; Morales, R. E. M.; Cameirão, A. A Multiscale Approach for Gas Hydrates Considering Structure, Agglomeration, and Transportability under Multiphase Flow Conditions: III. Agglomeration Model. *Ind. Eng. Chem. Res.* **2020**, *59* (34), 15357–15377. https://doi.org/10.1021/acs.iecr.0c02633.

(2) Brauner, N. The Prediction of Dispersed Flows Boundaries in Liquid-Liquid and Gas-Liquid Systems. *Int. J. Multiph. Flow* **2001**, *27* (5), 885–910. https://doi.org/10.1016/S0301-9322(00)00056-2.

(3) Kakitani, C. Experimental Study of the Gas Hydrate Formation upon Shut-in and Restart of Gas and Oil Pipelines (in Portuguese), PhD Thesis, Federal University of Technology - Paraná, Curitiba, Brazil, 2019.

(4) Bassani, C. L.; Melchuna, A. M.; Cameirão, A.; Herri, J.-M.; Morales, R. E. M.; Sum, A. K. A Multiscale Approach for Gas Hydrates Considering Structure, Agglomeration, and Transportability under Multiphase Flow Conditions: I. Phenomenological Model. *Ind. Eng.*

Chem. Res. **2019**, *58* (31), 14446–14461. https://doi.org/10.1021/acs.iecr.9b01841.

(5) Bassani, C. L.; Sum, A. K.; Herri, J.-M.; Morales, R. E. M.; Cameirão, A. A Multiscale Approach for Gas Hydrates Considering Structure, Agglomeration, and Transportability under Multiphase Flow Conditions: II. Growth Kinetic Model. *Ind. Eng. Chem. Res.* **2020**, *59* (5), 2123–2144. https://doi.org/10.1021/acs.iecr.9b04245.

(6) Bassani, C. L. A Multiscale Approach for Gas Hydrates Considering Structure, Growth Kinetics, Agglomeration and Transportability under Multiphase Flow Conditions. PhD Thesis, Federal University of Technology - Paraná in collaboration with Mines Saint-Etienne, 2020.